Ferroelectric–ferroelastic domain kinetic studies by deflection of light in an NH_4HSeO_4 crystal

2008 J. Phys.: Condens. Matter 20 175214

(http://iopscience.iop.org/0953-8984/20/17/175214)

J. Phys.: Condens. Matter **20** (2008) 175214 (6pp) doi:10.1088/0953-8984/20/17/175214

Ferroelectric–ferroelastic domain kinetic studies by deflection of light in an NH_4HSeO_4 crystal

P Staniorowski and S Dacko

Institute of Experimental Physics, University of Wrocław, Plac Maksa Borna 9, Wrocław, Poland

E-mail: piotr@ifd.uni.wroc.pl and dacko@ifd.uni.wroc.pl

Received 18 October 2007, in final form 26 February 2008
Published 7 April 2008
Online at stacks.iop.org/JPhysCM/20/175214

Abstract

Deflection of light studies of the ferroelectric–ferroelastic domain kinetics under the influence of an external electric field, applied to an NH_4HSeO_4 crystal sample, are presented. Splitting of the deflected A beam was observed in angular measurement for various states of sample polarization. It is also shown that the intensity of deflected beam A depends strongly on the electric field applied to the sample. Detailed studies of the deflected spot intensity were performed. Our calculations allowed us to establish a correlation between domain wall density, controlled by the electric field, and deflection intensity.

1. Introduction

Ammonium hydrogen selenate—NH_4HSeO_4 (abbreviated as AHSe)—is a well known ferroelectric crystal in which successive phase transitions have been observed [1–4, 15]. At room temperature the crystal is monoclinic and belongs to polar class 2. Its pseudo-orthorhombic unit cell with a symmetry $I2$ and monoclinic angle equal to 90.73° is chosen to describe some physical properties of the crystal. In some as-grown crystals natural twinning in the plane (100) of the pseudo-orthorhombic crystallographic system of the AHSe crystal was occasionally observed at room temperature. On cooling the crystal undergoes phase transitions to a modulated phase at 261 K and to a ferroelectric phase at 250 K. Below 250 K the AHSe crystal belongs to the triclinic system. The change of crystallographic system from monoclinic to triclinic gives a ferroelastic–ferroelectric domain structure with domain walls in the plane (001) [6, 7]. The ferroelastic domain structure was found to give deflection of light [5, 8–13, 20, 21]. A schematic description of deflection phenomena is presented in figure 1.

Light deflection should not be confused with another optical phenomenon casually occurring in some ferroelastic materials—diffraction of light passing through the ferroelastic structure [18, 19]. A number of conditions must be fulfilled to observe such diffraction. (1) The angle between optical indicatrices in adjacent domains should be approximately equal to 90° (as in GMO or KDP crystals). (2) The light intensity distribution of the diffraction spots has the well known, typical form. (3) Spot number is generally unlimited and the angular distance between them is constant and independent of the incidence angle. (4) All diffraction maxima are linearly polarized. None of these conditions is fulfilled in the AHSe crystal.

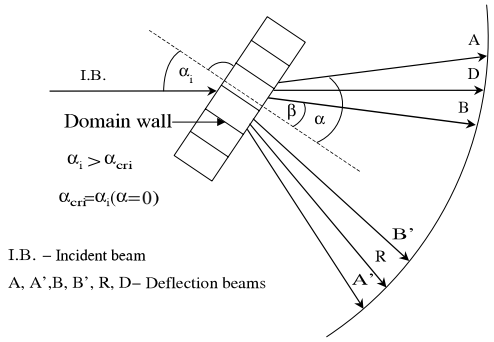

Figure 1. Scheme of the deflection phenomenon.

As can be seen, the incident beam crossing the sample divided into ferroelastic domains is split into several beams at its output. Below 250 K the strong dependence of deflected light intensity on the electric field applied to the sample in ferroelastic–ferroelectric phase was observed [14]. The aim of

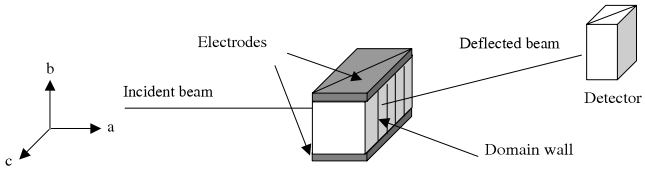

Figure 2a. Scheme of the experimental layout.

the present paper is to study in detail this dependence for light incidence at the plane (100), to get information about domain structure changes in correlation with the state of macroscopic, ferroelectric polarization in AHSe crystals.

2. Experimental details

Single crystals of AHSe were grown from saturated water solution containing polycrystals of AHSe with some excess of selenic acid by the slow evaporation method at a constant temperature of 304 K. Single, monoclinic at room temperature, domain seeds were used to obtain samples for deflection studies in the triclinic phase (which exists below 250 K). The sample was prepared in the form of a rectangular plate of dimensions $3 \times 2 \times 1$ mm^3—$c \times b \times a$. It was mounted on the sample holder giving the possibility to cool and rotate it with respect to the incident laser beam step by step. The He–Ne laser of 633 nm was used as a light source. Deflection of light was measured using a system that allowed us to measure the angle of deflection with an accuracy of 0.01° and relative intensity with an accuracy of 1%. In the first experiment, the angular intensity distribution of the deflected spot A was observed in the plane (001). In the second experiment, the deflection intensity was measured as a function of the external electric field applied in the b-direction (figure 2a).

3. Results and discussion

3.1. Structure of the deflected spot

In some experiments the angular splitting of the deflected beam (spot) was observed. To get information about the structure of the deflected spot we studied the intensity changes of the central part of the spot as a function of sample polarization state. Changes of the polarization from one state to another were induced by changes of the low frequency electric field ($f = 1 \times 10^{-2}$ Hz, $E_{\max} = 2 \times 10^5$ V m^{-1}). Polarization changes were measured using an electrometer. During each angular scan procedure, this field was switched off (or maintained at a constant small value) to stabilize the domain structure ($P_m = \text{const}$). We measured the distribution of the A spot intensity in the range of ±0.70° with respect to the center of the spot, which appears at the angle 24.8°. The slot of the photodiode allowed us to measure in every position about 10% of the angular width of deflected spot. During measurement we changed the position of the photodiode and scanned intensity changes of the spot. These measurements were made for various polarization states of the sample. The results are presented in figures 3(a)–(c). As can be seen in this figure, each single angular maximum is divided into two submaxima. These two maxima of the deflection peak are related to spontaneous strain which appears at the transition from monoclinic to triclinic phase. At this transition, domains appear with opposite polarization and opposite strain. This results in a small change of the beam incident angle on positive and negative domains. In this way both positive and negative domains give their own contribution to total deflected spot intensity (figure 2b). The change of polarization state (with electric field) gives a change of the positive and negative domain contributions to the intensity. This is possible only if both parts of the spots depend on the electric field (polarization state).

It is easy to show that $\Delta\alpha_d = \alpha_2 - \alpha_1 = \alpha'' - \alpha' - 2\Delta\beta$, where $\alpha' = \arcsin[n_t \sin(\theta - \Delta\beta)]$, $\alpha'' = \arcsin[n_t \sin(\theta + \Delta\beta)]$, n_t is the refraction index in a specific light propagation direction and θ is a refraction angle on the domain wall. Calculations done on the basis of the above formulas give as a result $\Delta\alpha = 0.35°$ for $\alpha_i = 0°$. This value is greater than the observed one ($\Delta\alpha_{\text{exp}} \approx 0.20°$). We suppose that small surface imperfections can be a possible explanation for this discrepancy. However, a more satisfactory response requires further detailed studies. The contribution of both main maxima

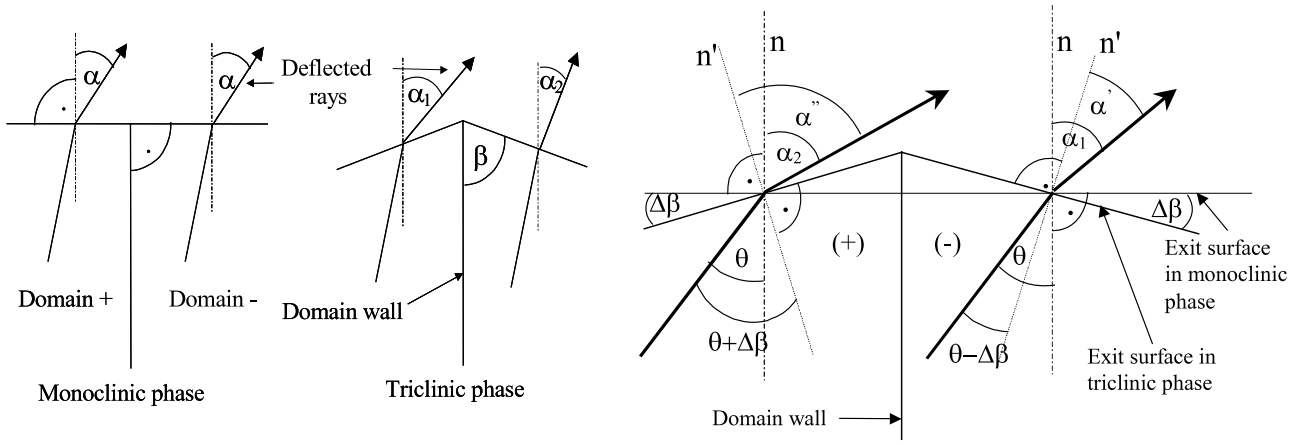

Figure 2b. General view of the spontaneous strain influence on the deflection angle α, in a triclinic phase. α', α''—deflection angles, β—strain angle = 89.03° in the triclinic phase.

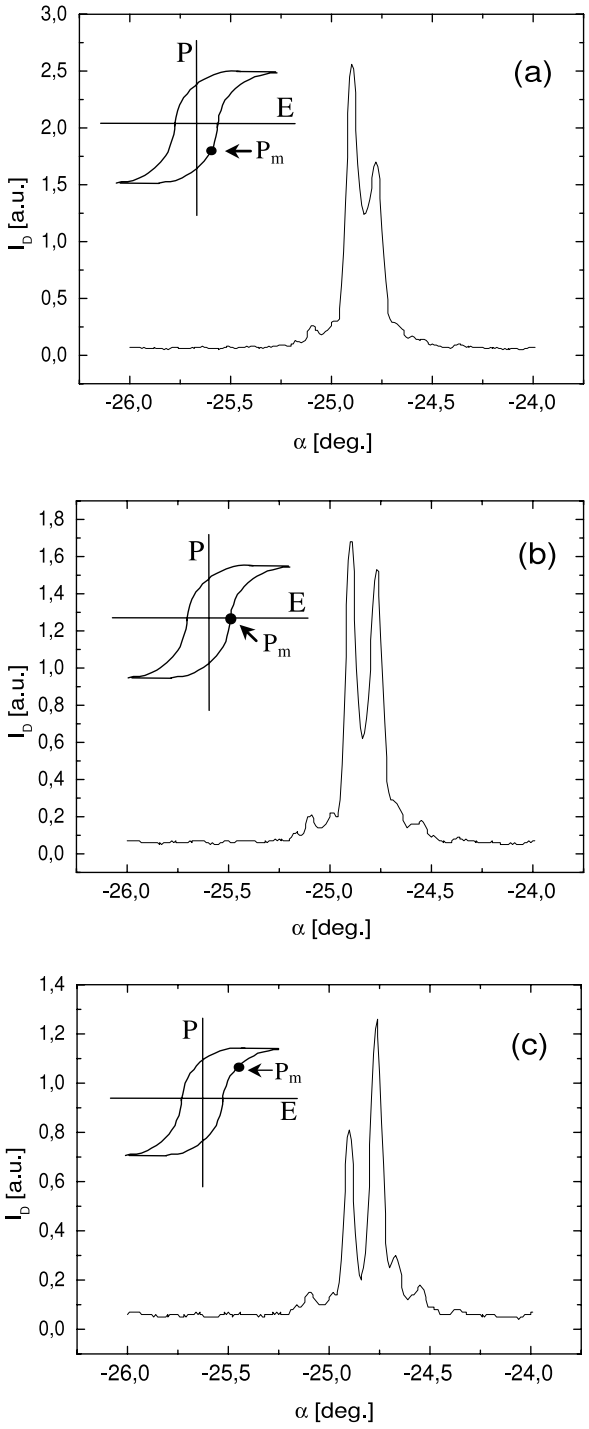

Figure 3. Angular structure of the deflected A spot in three different polarization states; $T = 240$ K.

to the total intensity of the deflected spot changes considerably with the polarization state changes. For degree of polarization $0 < |P_m| \prec 0.25P_s$ the intensity is still high but the relative height of both peaks is changed. The intensities of both peaks for P_m close to zero are nearly equal. For $P_m \approx +0.14P_s$ and $-0.14P_s$ (P_s corresponds to the saturation state and values 0.14 and 0.25 are taken from the hysteresis loops), the intensities of both maxima change their heights. This observation can be explained by the change of domain number with reversed spontaneous strain, which causes a different deflection angle and a change of main maximum height of the deflected spot (see above). For bigger polarization degree, the main maxima become smaller, which generally gives a decrease of the total intensity of the deflected A spot connected with the decrease of domain wall number. As can be seen in figure 3, additional weaker local maxima on both sides of the main one are observed, which are probably connected to the additional interference and diffraction effects.

3.2. Deflection intensities versus external electric field

(1) The deflection intensity as a function of the applied electric field and related hysteresis loops for deflected beams at several temperatures are shown in figures 5a, 5b and 6a, 6b. The incidence angle for cases A and B was 30°. The dependences show hysteresis characteristic for the ferroelectric phase with the main maximum intensity observed for electric field close to the coercive field ($\pm E_c$). In a previous paper [14] we have explained it roughly as a result of correlation between the domain wall density taking part in the light deflection and the sample polarization state. However, a complementary effect—the splitting of each maximum into several submaxima—was observed. The same behavior was evidenced for both A and B spots.

(2) The detailed shape of each maximum depends on temperature (figures 5a, 5b and 6a, 6b). In our experiment, electric field changes at a rate of $dE/dt = \pm 8 \times 10^3$ V m^{-1} s^{-1}. Then, intensity peaks become wider and are split at lower temperature.
This can be explained using a general description of the ferroelectric/ferroelastic domain wall dynamics.

Ferroelastic crystal switching is a multi-step process. It can be described as follows: (1) nucleation of domains with opposite polarization states; (2) domains growth through the crystal; (3) domain volume increasing due to the side motion of domain walls.

Starting from the monodomain state, one can describe the domain nucleation process by the following expression:

$$\frac{dN}{dt} \propto e^{-\frac{\alpha_1}{E}}$$

where dN is the number of domain nuclei, E the intensity of the applied electric field and α_1 a constant.

Domains growth through the sample seem to be crucial at the first Stage, which corresponds to the deflection intensity increasing. It can be described as follows [16]:

$$v_y \propto E^n \tag{1}$$

where v_y is the growth velocity and $n = 1$, in the first approximation. A decrease of the number of domain walls taking part in the deflection pattern creation is induced mainly by the side motion of domain walls, during coalescence, sweeping them out the region 'seen' by the laser beam. It plays a main role in the second stage (decreasing of the

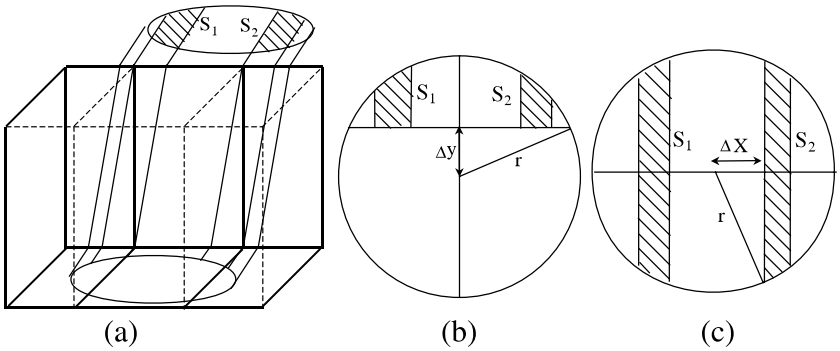

Figure 4. 3D exemplification of the incident beam areas ('shadows' of the domain walls on the incident beam plane) taking part in deflection for two domain walls (a). Scheme of such areas in the first stage (domain wall growth) (b) and the second one (domain wall lateral motion) (c). $S_1 + S_2 = S_{\text{ef}}$.

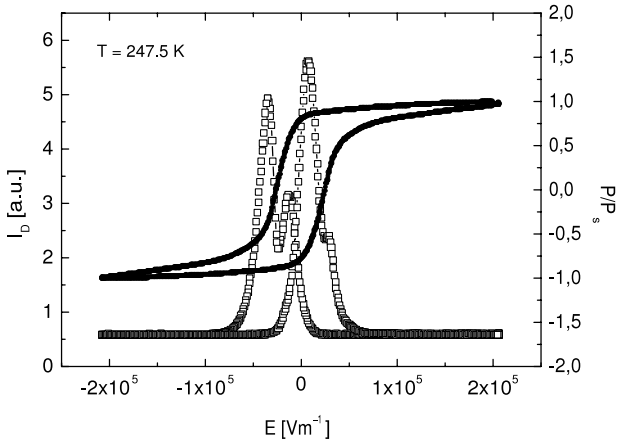

Figure 5a. The deflection intensity as a function of the applied electric field and related hysteresis loop for deflected beam A at $T = 247.5$ K—close to the phase transition.

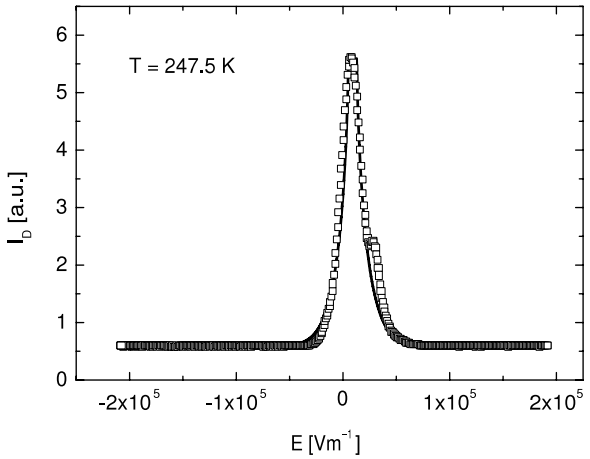

Figure 5b. Experimental data (squares) and theoretical predictions (continuous line) for chosen maximum at $T = 247.5$ K.

deflection intensity). This motion velocity can be described as follows [17]:

$$v_x \propto v_\infty \sum_n \mathrm{e}^{-\left(\frac{\alpha_2}{E}\right)n^{3/2}} \tag{2}$$

where v_∞ and α_2 are constants, n the thickness of the domain nucleus (in crystallographic lattice constants—usually $n = 1$) and E the electric field intensity.

Additionally, in the coalescence process, the starting moment of the walls' 'withdrawal' depends on the initial distance between approaching walls. The width distribution of domains occurring in the nucleation process (a Gauss distribution in the first approximation) will influence the decrease of the domain number in the laser beam incidence area.

Our proposal is to connect the velocity of domain wall growth with the applied field E by the equation

$$v_y = A(E \pm E_0) \tag{3}$$

in the first stage and the velocity of domain wall lateral motion with E

$$v_x = B\mathrm{e}^{-\left|\frac{a}{E \pm E_0'}\right|} \tag{4}$$

in the second one where A, B and a are constants, E_0 the electric field necessary for creation of the critically sized nucleus, and E_0' the electric field necessary for activation of the domain motion.

The relationship between domain wall motion and the deflected light intensity can be established. One can assume that deflection occurs and is reproduced successively on each following domain wall. The intensity of a given deflected beam is proportional to S_{ef}—the effective surface of the incident beam cross-section with domain walls:

$$\frac{I_D}{I_0} = k_D S_{\text{ef}} \tag{5}$$

where I_D/I_0 is the relative intensity, k_D the coefficient characteristic for a given deflected ray when the whole incident beam undergoes the deflection, and $S_{\text{ef}} = \sum S_i$ (figure 4(a)).

(1) We assume that ferroelectric switching from the monodomain state occurs mainly due to growing up nuclei located close to the electrode. Figure 4(b) corresponds to the occurring of domain walls in the observed (lit up by the incident beam) region. One can show that

$$S_{\text{ef}} \sim r^2 \arcsin\left(\frac{\Delta y}{r}\right) - \Delta y\sqrt{r^2 - (\Delta y)^2}$$

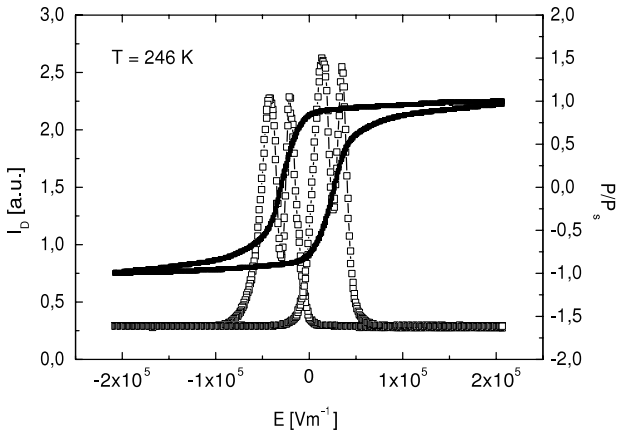

Figure 6a. The deflection intensity as a function of the applied electric field and related hysteresis loop for deflected beam A at $T = 246$ K.

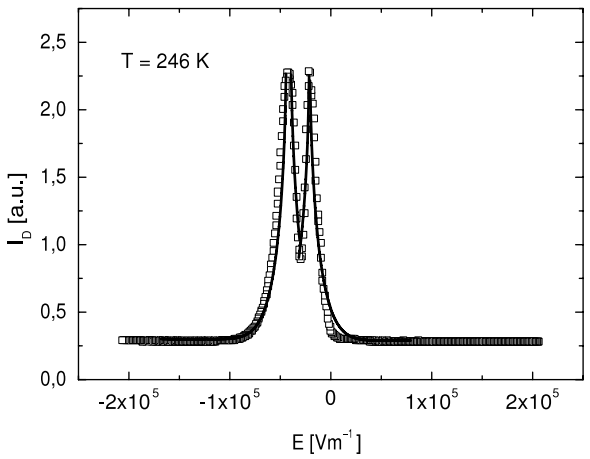

Figure 6b. Experimental data (squares) and theoretical predictions (continuous line) for chosen maximum at $T = 246$ K.

where growth velocity $v_y = \Delta y/\Delta t$. Because $\Delta E \sim \Delta t$ and $v \sim E$, we obtain $\Delta y = C_y(E - E_1)^2$, where C_y is a constant. From the above equations we obtain immediately

$$\frac{I_D}{I_0} = Ak_D\left[r^2 \arcsin\left(\frac{C_y(E-E_1)^2}{r}\right) - C_y(E-E_1)^2 \times \sqrt{r^2 - C_y^2(E-E_1)^4}\right] \quad (6)$$

where A, C_y, E_1 and k_D are to be fitted, $r \approx 0.35$ mm. As in our experiment the whole incident beam does not ever undergo the deflection, $A < 1$.

(2) In the second stage, decreasing of the domain wall density causes S_{ef} to decrease (figure 4(c)). Now

$$S_{\text{ef}} = \sum S_i = A'\left[r^2 \arcsin\left(\frac{\Delta x}{r}\right) - \Delta x\sqrt{r^2 - (\Delta x)^2}\right].$$

Because $v_x = \Delta x/\Delta t$ and $\Delta E \sim \Delta t$, we obtain from (4) and (5) that $\Delta x = C_x(E - E_2)\mathrm{e}^{-|\frac{a}{E-E_2}|}$. As in our case $E - E_2 \gg \delta E$ (δE is the range of the argument where deflection intensity decreases or increases—δE is small in comparison to the whole E range), so $\mathrm{e}^{-|\frac{a}{E-E_2}|}$ is practically linear in this range and $\Delta x \approx C_x(E - E_2)^2$. Finally,

$$\frac{I_D}{I_0} = k_D A'\left[r^2 \arcsin\left(\frac{C_x(E-E_2)^2}{r}\right) - C_x(E-E_2)^2 \times \sqrt{r^2 - C_x^2(E-E_2)^4}\right] \quad (7)$$

where A', C_x and E_2 are to be fitted. In formulas (6) and (7) we pass from discrete values of domain wall number to the continuous function of the electric field. This is well founded due to continuous wall appearance in the incident beam cross-section. These formulas with the above parameters ($C_x/r \approx C_y/r = 1.2 \times 10^{-10}$ V^{-2} m^2, $k_D A = 6.7 \times 10^{-18}$ m^{-2}, $k_D A' = 5.7 \times 10^{-18}$ m^{-2}, $E_1 = 0.6 \times 10^5$ V m^{-1}, $E_2 = 1.05 \times 10^5$ V m^{-1}) can be applied to explain the experimental data as shown in figures 5a and 5b.

Data presented in these figures were collected at a temperature relatively close to the transition point. Then the crystal becomes easily 'switchable' between two orientational states. This is why the domain sizes change gradually, without local and temporary inhomogeneities, and only two distinct maxima of deflected light intensity are observed. At lower temperatures ($T - T_c \approx 5$ K), local defects start to play a more important role, which can result in splitting of the main maxima, as shown in figures 6a and 6b.

Each of these maxima consists of two symmetric submaxima. They could correspond to the two types of processes for domain (and domain wall) change—appearance and disappearance. Appearance of one local domain structure would occur at the bottom of the sample while disappearance of the second structure would take place at the sample top, with a slight time shift. At a chosen moment walls number maximal domain density of one structure corresponds to the appropriate submaximum. Finally, such a complex double peak can be described as a sum of four processes given by the following equation:

$$\frac{I_D}{I_0} = k_D \sum_{i=1,2} A_i\left\{\left[br^2 \arcsin\left(\frac{C_{i,y}(E-E_i)^2}{r}\right) - C_{i,y}(E-E_i)^2\sqrt{r^2 - C_{i,y}^2(E-E_i)^4}\right] + \left[br^2 \arcsin\left(\frac{C_{i,x}(E-E_i')^2}{r}\right) - C_{i,x}(E-E_{0,i}')^2\sqrt{r^2 - C_{i,x}^2(E-E_i')^4}\right]\right\}. \quad (8)$$

Figure 6b shows good agreement between experimental data (dots) and the fitted curve (continuous line), obtained from equation (8). The case presented in figure 6a is a particular one because the two maxima are nearly equal. At temperatures more distant from the transition point ($T - T_c \approx 10$ K), the splitting of the main maxima is more

complex. This can be explained by the bigger number of activation fields existing in this temperature range, where each submaximum corresponds to one activation field E_{0i}. Such random domain activation can be analogous to Barkhausen jumps.

Generally, one can observe a certain deviation of the proposed fitting curve from experimental data for weak deflection intensities. We suppose this is connected to the situation where the domain size is comparable to the laser beam diameter. Then, even appearance of one or two domain walls causes an abrupt intensity increase, 'invisible' to our simplified model.

3.3. Summary

(a) In the present paper results of deflection intensity measurements for stabilized as well as for variable domain structure have been presented.
(b) It has been shown that the angular complexity of the deflection spot A was subsequent to ferroelastic deformation of the sample (crystal) surface.
(c) A model describing integral intensity of the A spot for the ferroelastic–ferroelectric crystal switching process has been proposed.

References

[1] Czapla Z, Lis T and Sobczyk L 1979 *Phys. Status Solidi* a **51** 609
[2] Krasikov V S and Kruglik A I 1979 *Fiz. Tverd. Tela* **21** 2834
[3] Czapla Z 1982 *Acta Phys. Pol.* A **61** 47
[4] Czapla Z, Pykacz H and Sobczyk L 1987 *Ferroelectrics* **76** 291
[5] Czapla Z, Dacko S and Guilbert L 2000 *Ferroelectrics* **237** 97
[6] Pykacz H, Mroz J and Czapla Z 1980 *Acta Phys. Pol.* A **60** 325
[7] Martynov V G and Anistratov A T 1982 *Fiz. Tverd. Tela* **24** 2013
[8] Tsukamoto T and Futama H 1993 *Phase Transit.* **45** 59
[9] Bornarel J, Staniorowski P and Czapla Z 2000 *J. Phys.: Condens. Matter* **12** 653
[10] Staniorowski P and Bornarel J 2000 *J. Phys.: Condens. Matter* **12** 669
[11] Kolata P, Guilbert L, Fontana M D, Salvestrini J-P and Czapla Z 2000 *J. Opt. Soc. Am.* B **17** 1973
[12] Fujii Y, Yoshioka S and Kinoshita S 2004 *Ferroelectrics* **303** 55
[13] Fujii Y, Yoshioka S and Kinoshita S 2006 *Ferroelectrics* **334** 11
[14] Staniorowski P, Dacko S and Czapla Z 2002 *Ferroelectrics* **272** 3
[15] Andrievskii B, Czapla Z and Myshchyshyn O 1998 *Phys. Status Solidi* a **165** 495
[16] Little E A 1955 *Phys. Rev.* **98** 978
[17] Miller R C and Weinreich G 1960 *Phys. Rev.* **117** 1460
[18] Hill R M and Ichiki S K 1964 *Phy. Rev.* **135** 1640
[19] Ha D-H and Kim J-J 1985 *Japan. J. Appl. Phys.* **24** (Suppl. 24-2) 556
[20] Goulkov M, Granzow T, Dörfler U, Woike Th, Imlau M, Pankrath R and Kleemann W 2003 *Opt. Commun.* **218** 173–82
[21] Dieckmann V, Selinger A, Imlau M and Goulkov M 2007 *Opt. Lett.* **32** 3510